Nuclear Inst. and Methods in Physics Research B 461 (2019) 77–82

Contents lists available at ScienceDirect

Nuclear Inst. and Methods in Physics Research B

journal homepage: www.elsevier.com/locate/nimb

Depth profiles of damage creation and hardening in MgO irradiated with GeV heavy ions

I. Manika[a,*], J. Maniks[a], R. Zabels[a], R. Grants[a], A. Kuzmin[a], K. Schwartz[b]

[a] Institute of Solid State Physics, University of Latvia, 8 Kengaraga str., LV-1063 Riga, Latvia
[b] GSI Helmholtz Centre for Heavy Ion Research GmbH, 1 Planckstr, 64291 Darmstadt, Germany

ARTICLE INFO

Keywords:
MgO crystals
Swift heavy ions
Dislocations
Nanoindentation
Photoluminescence

ABSTRACT

The effect of irradiation with GeV heavy ions (U, Au, Bi) on the structure and mechanical properties of MgO single crystals was studied. The methods of nanoindentation, dislocation mobility, optical absorption and photoluminescence (PL) spectroscopy, X-ray diffraction and atomic force microscopy were used for damage characterization. The ion-induced increase of hardness and reduction of dislocation mobility was observed. The depth profiles of hardness, dislocation mobility and PL were investigated, and the contribution of electronic and nuclear loss mechanisms was confirmed. The efficiency of damage *vs.* average absorbed energy for heavy and light ions was compared. The change in the mechanism of plastic deformation at indentation was observed after severe irradiation due to the immobilization of dislocations by ion-induced extended defects. The results show that MgO single crystals maintain integrity and micro-plasticity at indentation, and exhibit improved hardness after irradiation with swift heavy ions at fluences up to 7×10^{13} ions/cm^2.

1. Introduction

MgO single crystals exhibiting high radiation and thermal resistance are promising as a construction material for nuclear and related applications. Therefore, acute issues are applicability studies of radiolysis-resistant refractory oxides, such as MgO, under conditions of severe irradiation with high-energy particles, in particular, with swift heavy ions (SHI), energy losses of which are of the same order of magnitude as for fragments of nuclear fission.

The basic criteria for technological applications include not only suitability of functional properties but also the ability to maintain mechanical integrity and acceptable plasticity under severe irradiation. MgO is known as a brittle material under conditions of macroscopic deformation at room temperature but exhibits significant plasticity under local deformation at the micro- and nano-scale.

Much effort in the radiation damage studies of MgO, MgO-based spinels and related ionic crystals was devoted to the formation of primary radiation defects and their aggregates [1–8]. It is well established that irradiation with SHI at the stage of track overlapping creates also defect clusters and extended defects, such as dislocations [9–12].

Defect aggregates and extended defects play an important role in the mechanical properties of irradiated ionic crystals, while the single defects are of minor importance [13]. The most prominent extended defects are ion-induced nano-size dislocation loops whose presence in MgO under different types of irradiation (neutrons, electrons, swift ions) is revealed in numerous studies using transmission electron microscopy (TEM) technique [5,9,10,14–16]. The nanoindentation method as a local probe sensitive to the presence of dislocations and aggregate defects can be effectively used in investigations of the evolution of extended defects [13,17].

A number of publications are devoted to the investigation of dislocation structures produced during micro- and nanoindentation [18,19]. However, the role of ion-induced dislocations in the modification of mechanical properties and the evolution of dislocation structures along the ion path under conditions of severe irradiation are poorly understood.

In our recent study, the depth profiles of damage and hardening in MgO single crystals irradiated by relatively light ions (N and Kr) were studied [20]. The role of dislocations and the contribution of electronic excitation and elastic collision mechanisms to damage was considered. Here we extend our study to GeV energy heavy ions, such as U, Bi, and Au, which have high energy loss in MgO (up to 38 keV/nm) and higher potential to produce damage and modify properties.

2. Experimental

The samples of MgO single crystals (MTI, Ca, USA) with a purity of 99.85% (the main impurities: Ca (0.13%), Fe, and Cr) were prepared by

* Corresponding author.
E-mail address: ilze.manika@cfi.lu.lv (I. Manika).

https://doi.org/10.1016/j.nimb.2019.09.026
Received 24 July 2019; Received in revised form 27 August 2019; Accepted 16 September 2019

Table 1
Irradiation parameters of MgO single crystals.

Ions	Ion energy, MeV	Range, μm	Fluence, ions/cm^2
^{238}U	2046	56	10^{13}
^{209}Bi	1003	34.8	5.10^{11}–5.10^{12}
^{209}Bi	2150	67	10^{12}
^{197}Au	2187	72	5.10^{12}–7.10^{13}
^{84}Kr [20]	147	13	5.10^{12}–10^{15}

cleaving of crystals along (1 0 0) crystallographic planes to the thickness of about 1 mm and the size of about 10 × 10 mm^2. The crystals were irradiated at the UNILAC of GSI, Darmstadt with GeV energy U, Au, Bi and Kr ions at fluences 5 × 10^{11}–7 × 10^{13} ions/cm^2 (Table 1). The irradiations were performed at room temperature and at nearly normal incidence of the ion beam to the (1 0 0) face of crystals. In selected experiments, the grazing incidence of ion beam at 50° against the normal was also used. The energy loss and the range of ions were calculated using SRIM 2008.04 [21]. The ion range was in all cases less than the sample thickness, thus the ions were stopped within the crystal.

X-ray diffraction (XRD) and optical spectroscopy were used for the characterization of ion-induced damage. The depth profiles of color centers were studied by a confocal laser scanning spectromicroscopy using continuous-wave laser excitation (532 nm, max power 150 mW) and spectroscopic registration of the color center photoluminescence emission (PL) at a wavelength around 760 nm. The accuracy of the depth measurements was 0.5 μm. The experimental details can be found in Ref. [22].

The evolution of extended defects was studied by nanoindentation, dislocation mobility and chemical etching techniques. Ion-induced changes of micro-mechanical properties were characterized by the Nanoindenter G200 (Agilent, USA) equipped with Berkovich and Vickers diamond tips. Measurements were performed in ambient air at room temperature using the standard (BASIC) and continuous stiffness (CSM) measurement techniques. The nanoindenter was calibrated using a reference sample of fused silica. The hardness, Young's modulus and standard deviation of the measurements were calculated from experimentally obtained loading/unloading curves by means of the Oliver-Pharr method [23]. The obtained results were averaged from 10 individual measurements. The depth profiles of hardness and modulus were measured on surfaces prepared by cleaving the samples along the direction of an ion beam. The measurements were performed at a constant indentation depth (150 nm) ensuring small indents and a reasonable amount of data points with good statistics (average standard deviation 0.16 GPa). The distance of indents from the irradiated surface corresponding to the penetration depth of ions was measured by optical microscopy with an accuracy of 1.5 μm. The ion-induced effect was expressed as the relative variation of hardness: $(H\text{-}H_0)/H_0$, where H_0 and H is the hardness of non-irradiated and irradiated crystal, correspondingly. Taking into account the size effect in indentation hardness [24], the hardness tests on pristine and irradiated samples were performed at the same indentation depth.

The indentation hardness tests were complemented with the measurements of dislocation mobility [13]. The relative variation of dislocation arm length around imprints $(l_0\text{-}l)/l_0$ served as a parameter quantitatively characterizing the effect of dislocation braking on ion-induced defects as obstacles. Ion-induced and indentation-induced dislocations were revealed by a short time (5 s) selective chemical etching in a hot aqueous $FeCl_3$ solution [25] and subsequent imaging by atomic force microscopy (AFM) in the tapping mode.

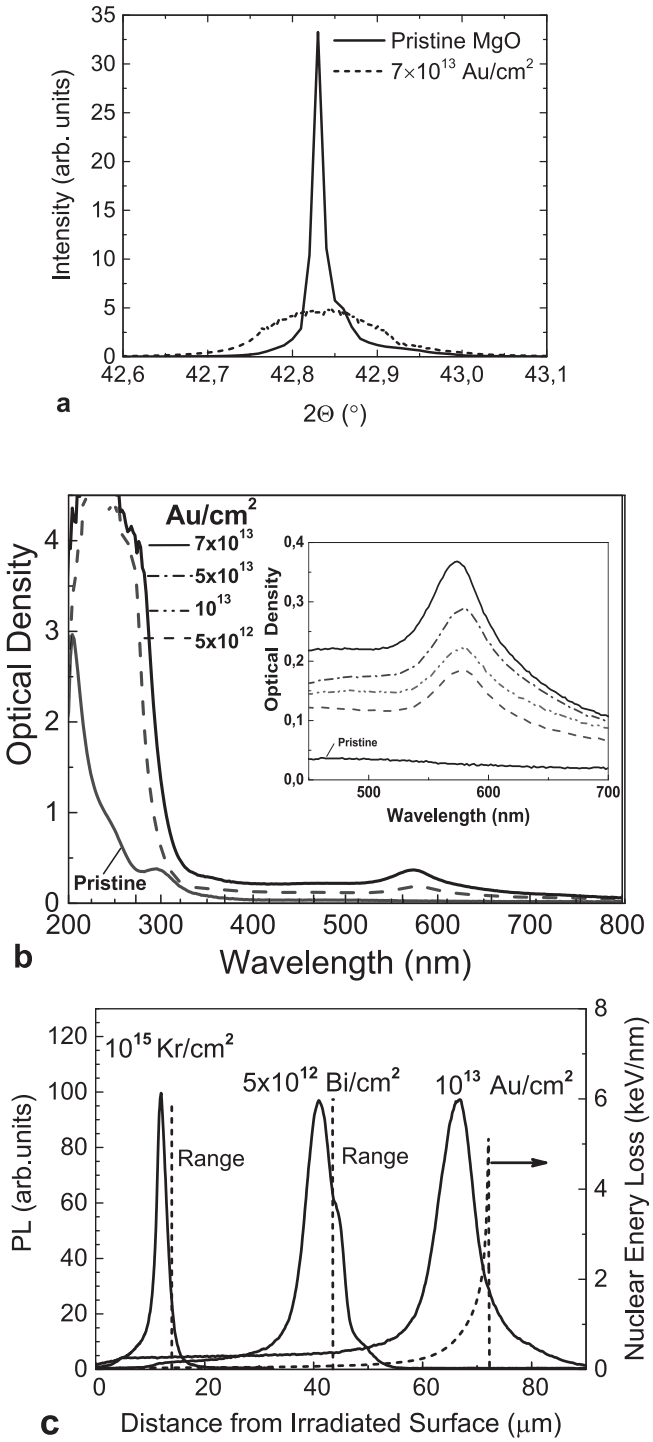

Fig. 1. XRD (a), optical absorption spectra (insert shows the effect of fluence on 575 nm band absorbance for 2.2 GeV Au ions) (b) and the depth profiles of laser-excited red photoluminescence for MgO irradiated with different ions (c).

3. Results and discussion

3.1. XRD, optical and photoluminescence spectroscopy

XRD data of pristine and ion-irradiated crystals in the range of MgO (2 0 0) reflection confirm the crystallinity of irradiated samples (Fig. 1a). However, the broadening of the (2 0 0) peak in samples exposed to severe irradiation (2.2 GeV Au, $\Phi = 7 \times 10^{13}$ ions/cm^2) indicates the accumulation of ion-induced structural defects in significant concentration.

The optical absorption spectra of MgO irradiated with swift Au and U ions (Fig. 1b) consist of a strong band at 250 nm assigned to a large amount of ion-induced neutral and charged oxygen vacancy centers (F^+ and F type centers), a weak band at 355 nm ascribed to complex color centers (F_2), and the band at 575 nm due to unidentified aggregate defects. The insert shows the effect of fluence on evolution of 575 nm band for Au ions. This band is also well-established in the absorption spectra of neutron-irradiated crystals [26–29]. Neutrons are stopped in solids mainly by elastic collision (nuclear) mechanism.

The aggregate color centres are of interest due to their possible involvement in the modification of mechanical properties. In order to obtain depth profiles of defect aggregates absorbing at 575 nm, the PL measurements were performed on freshly prepared MgO surfaces using a confocal laser scanning spectromicroscopy at 532 nm cw laser excitation. The wavelength curve of PL emission for irradiated crystals displays a broad complex peak at 760 nm. Fig. 1c shows the variation of PL along the ion path for samples irradiated with Kr, Bi and Au ions, which have different penetration depth. The maximum of PL is observed at the end-of-range region where nuclear energy loss of ions reaches the maximum (as shown for Au ions). The intensity of PL is low in the remaining part of range where the electronic stopping mechanism plays the dominating role. The result confirms that the highest concentration of luminescent aggregate defects at given fluences is located in the tail part of range. Such result is not surprising taking into account that the contribution of nuclear stopping mechanism in the case of swift heavy ions is of importance only in the tail part of the ion range. The similarity of damage processes here with those in neutron-irradiated MgO can be expected.

The luminescence measurements give no full information about the concentration of the aggregate centers we are looking for. The evolution of structural damage during irradiation possibly could involve concentration quenching of luminescence and stress-promoted non-radiative decay processes as it was observed for luminescent F_3^+ and F_2 centers in radiation sensitive LiF crystals [30]. However, it should be noted that the PL signal in our experiments (Fig. 1c) is comparatively strong and almost independent of fluence (5.10^{12} Bi/cm^2, 10^{13} Au/cm^2 and 10^{15} Kr/cm^2) thus showing no indications of luminescence quenching in the investigated range of doses.

3.2. The depth profiles of hardness in ion-irradiated MgO

The hardness tests were performed on profile surfaces obtained by cleaving the irradiated crystals along the direction of ion beam. An optical micrograph of the profile surface reveals the irradiated zone as a striped structure oriented along the direction of the ion beam (Fig. 2a). The depth of the etched zone nearly coincides with the ion range calculated by SRIM. The micrographs indicate also the presence of swelling-induced stresses that can affect the evolution of damage structures. The long-range bending stresses at high fluences can exceed the dislocation yield stress and relax by the formation of dislocation slip lines on $(1\,1\,0)_{45}$ planes as it was observed earlier for ion-irradiated LiF crystals [31]. Besides, the shear stress arises along the interface between irradiated and non-irradiated parts of the crystal, which manifests as a bright zone in the polarized light (Fig. 2b).

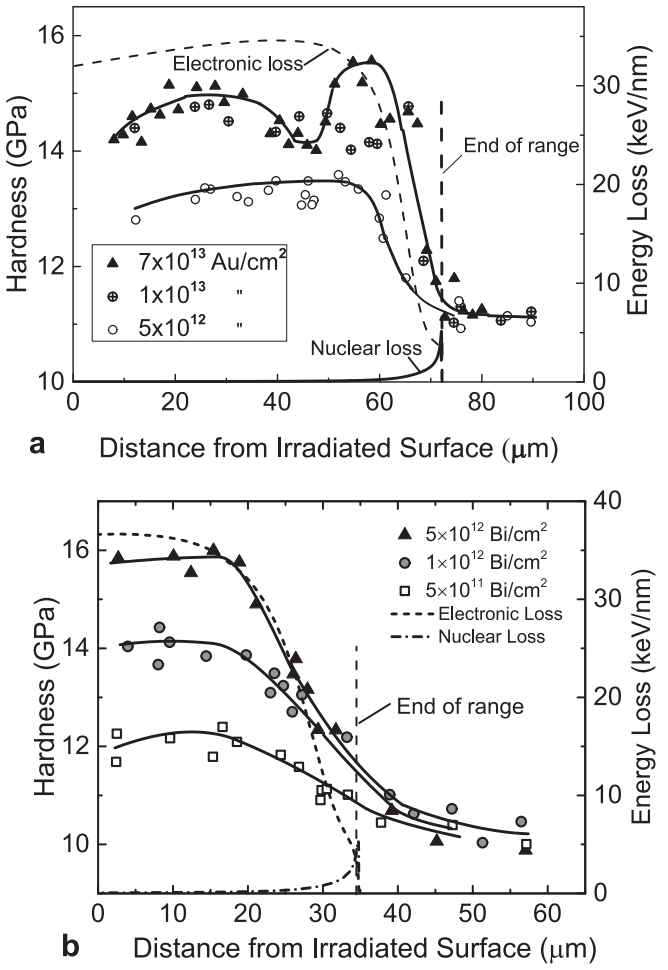

Fig. 3. Depth profiles of hardness and calculated energy loss in MgO samples irradiated with 2.2 GeV Au (a) and 1 GeV Bi ions (b) at different fluences.

The depth profiles of hardness in samples irradiated with GeV energy Au and Bi ions at different fluences are shown in Fig. 3. The increase of hardness is observed at fluences corresponding to the stage of track overlapping. The hardness increases with increasing the fluence (Φ) and begins to saturate at $\Phi > 10^{13}$ ions/cm^2. The hardness at saturation reaches an upper limit (H = 15–16 GPa, hardening effect

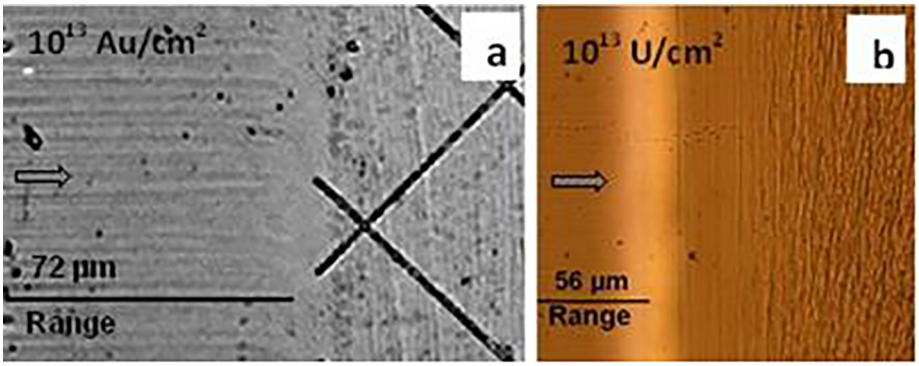

Fig. 2. Optical micrograph of the profile surface of irradiated crystal (after etching) (a), the zone of swelling-induced shear stress (in polarized light) (b). The direction of an ion beam is indicated by arrows.

40–45%). In the major part of ion range, the depth profile of hardness correlates with the depth behavior of calculated electronic energy loss. An exception is the end-of-range region where the hardened zone at $\Phi = 7 \times 10^{13}$ ions/cm^2 becomes broadened towards the end of range and the hardening effect even displays a second maximum (Fig. 3a) that points to the significant contribution of the nuclear stopping mechanism to damage. No or small contribution of the nuclear mechanism to hardening was observed at $\Phi < 10^{12}$ ions/cm^2.

The indentation plasticity in ion-irradiated MgO was calculated from the loading-unloading curves obtained by nanoindentation tests [23]. The results for pristine crystals show comparatively high microplasticity (~72%). A slight reduction of plasticity is observed in irradiated samples. However, even after irradiation with the highest fluence (7×10^{13} Au/cm^2) the indentation plasticity remains high enough (66%). The Young modulus calculated from the nanoindentation data in pristine crystals was about 340 GPa. In irradiated crystals, the modulus increased, however, the magnitude of the effect was small (few %).

3.3. Dislocation mobility in ion-irradiated MgO

Hardness tests were complemented with measurements of dislocation mobility [13,20]. Dislocation structures generated during micro- and nano-indentation tests in MgO have been studied in detail in [19, and references therein]. It is well established that indentation on a (1 0 0) surface creates four dislocation wings which belong to ⟨1 1 0⟩ {1 1 0}$_{45}$ slip system with slip planes inclined at 45° to the (0 0 1) surface and four dislocation wings which belong to ⟨1 1 0⟩{1 1 0}$_{90}$ slip planes oriented perpendicular to the (0 0 1) surface.

The pattern of indentation-induced dislocations in pristine and irradiated MgO was revealed by etching. A view of the dislocation rosette around the Vickers imprint on (0 0 1) surface of pristine MgO is shown in Fig. 4a, where four longer arms belong to half-loops of edge dislocations and four shorter – to screw dislocations. The relative variation of the length of edge dislocation arms was used in the measurements of dislocation mobility. The screw dislocations are more sensitive to radiation defects, and their arms disappear already at moderate fluences (Fig. 4b).

The measurements of dislocation mobility showed a decrease in the dislocation arm length for irradiated MgO (Fig. 4b) due to the braking of dislocations by radiation defects as obstacles. The effect increases with the fluence and for the ions used turns to saturation at the fluences above 5×10^{12} ions/cm^2.

The comparison of the depth profiles shows that dislocation mobility is more sensitive to structural damage than the indentation hardness. Its magnitude at saturation exceeds 70% while the ion-induced hardening reaches about 45% (Fig. 5). At moderate fluences, the depth profiles of dislocation mobility correlate with the depth behavior of calculated electronic energy loss.

Under conditions of severe irradiation, the appearance of the deformation zone around indents changes radically (Fig. 4c). The

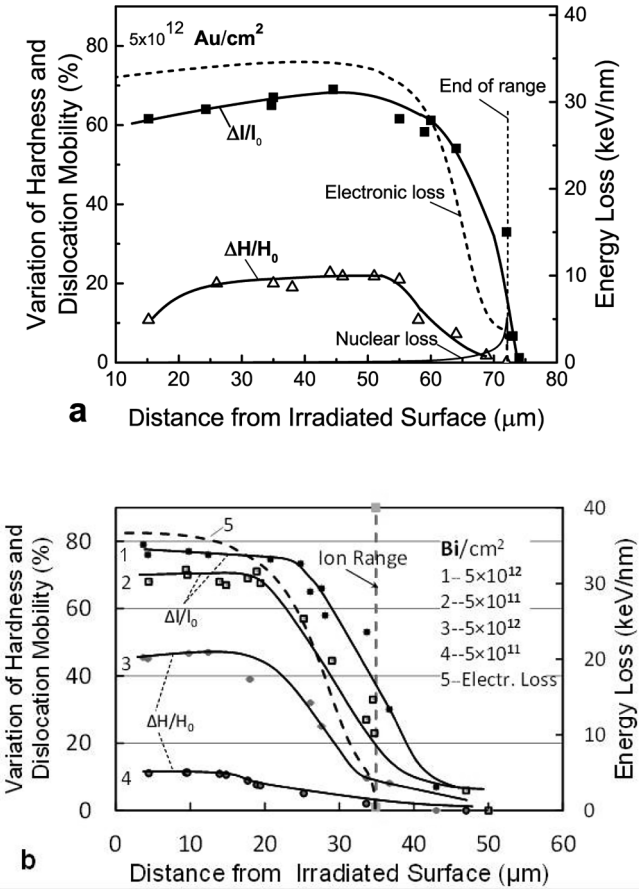

Fig. 5. The relative variation of hardness, dislocation mobility and energy loss along the ion path in MgO irradiated with Au (a) and Bi ions (b).

evolution of deformation zone no longer follows the crystallographic directions of dislocation slip but coincides with the stress distribution around the indenter where the maximum stress appears against the centres of indenter faces as it is observed at indentation on amorphous materials. The result gives an evidence of the exhaustion of the dislocation mechanism of plastic deformation in heavily irradiated MgO and of the involvement of a non-dislocation mechanism of deformation. Such change of the deformation mode in ion-irradiated MgO was observed earlier at multi-cycling nanoindentation and the involvement of a point-defect assisted deformation mechanism was suggested [32]. Some contribution of such mechanism was detected already in pristine MgO [33]. A similar change of the deformation mechanism was observed earlier for ion-irradiated LiF [29,34].

The depth profiles of hardness and dislocation mobility (Fig. 3 and

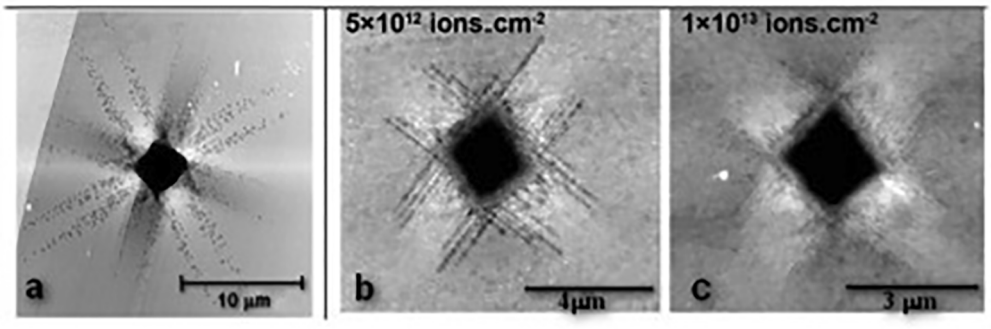

Fig. 4. Dislocation rosette around Vickers indents on a pristine crystal (a) and appearance of the deformation zone on samples irradiated with Au ions at different fluences (b and c) (after etching).

Fig. 5) confirm the dominating role of the electronic stopping mechanism of damage in the major part of ion range despite to the fact that the formation energy of Frenkel pairs in MgO is higher than the energy gap ($E_{FD} > E_g$) and the energetic criterion for electronic excitation mechanism of damage is not fulfilled. Alternative electronic excitation and ionization mechanisms of Frenkel defect formation in MgO based on the recombination of hot conduction electrons with hole traps or with the holes localized at impurity ions were offered [2,11]. Favorable conditions for the ensuring of such mechanisms - the presence of impurities (Ca, Fe and Cr) and ultimate excitation of an electronic subsystem along the tracks [3] – are met also in our experiments. In turn, the formation of extended defects by the nuclear mechanism clearly manifests in the tail part of range as evidenced by the hardness, dislocation mobility and photoluminescence data.

The results of TEM studies confirm that nano-size dislocation loops of interstitial type having the Burgers vector $b = a/2$ [1 1 0] and lying on {1 1 0} planes are created in MgO and related ionic crystals under different kinds of irradiation, including electrons, neutrons and ions [1,4,5,9,10,14–16]. The damage by SHI is localized in tracks [12]. The formation of dislocations in track periphery is observed by TEM [15,17,35]. An intense accumulation of dislocations occurs at the stage of track overlapping.

In the present study, the ion-induced dislocations in MgO were revealed by chemical etching. The etching procedure was successful for revealing the dislocation loops created at indentation (Fig. 4). Nevertheless, the quality of chemical etching of ion-induced dislocation loops in MgO was rather poor due to the small size of dislocations and chemical activity of irradiated surfaces at etching. To reveal dislocations in ion tracks, the experiments were performed on MgO samples irradiated with Bi ions, the energy loss of which is well above the critical 22 keV/nm threshold for formation of continuous etchable tracks. The samples were irradiated under normal and 50° incidence of the ion beam. The results show that in both cases the dislocations (dark etch pits) are ordered in rows along the ion path (Fig. 6) similarly as observed for ion-irradiated LiF crystals above the critical 10 keV/nm threshold of electronic energy loss [19,36]. The ion range along the direction of the ion beam for both irradiation angles was practically the same.

3.4. The comparison of the damage efficiency by heavy and light ions

In order to compare the ion-induced effects in MgO by ions with a different mass, energy and fluence, the dependence of hardening is plotted as a function of average absorbed energy estimated as $E_a = E_{ion} \times \Phi/R$ where E_{ion} is the energy of incoming ions, R is the ion range, and Φ is the fluence. The hardness data for each ion at a given fluence were taken from the depth profile curves at the position, which nearly corresponds to the Bragg maximum of electronic energy loss.

The results for heavy ions show an increase of the hardening effect at absorbed energies above 10^{23} eV/cm^3 followed by a saturation stage above 10^{24} eV/cm^3 at which the hardening effect approaches ~40%

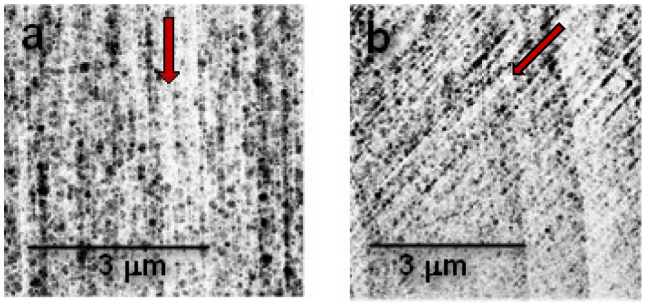

Fig. 6. View of dislocation rows along ion tracks on (0 0 1) face for samples irradiated with 2.1 GeV Bi ions under normal (a) and 50° incidence (b) of the ion beam. $\Phi = 10^{12}$ Bi/cm^2. Arrows denote the direction of ion beam.

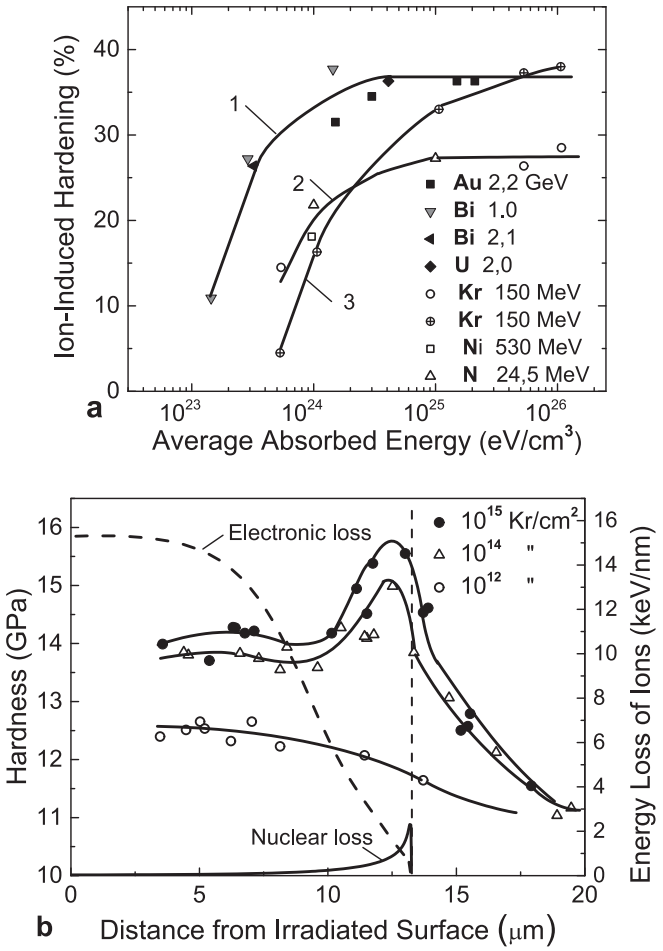

Fig. 7. (a) Effect of ion-induced hardening of MgO on average absorbed energy for heavy ions (Au, Bi, U – curve 1) and lighter ions (Kr, N – curves 2 and 3). (b) Depth profiles of hardness for Kr ions at different fluences (data from Ref. [20]).

(Fig. 7a, curve 1). The hardening data for lighter ions (Kr and N) (Fig. 7a, curve 2) were taken from our previous results [20]. In this case, the hardening effect is initiated at an order of magnitude higher average absorbed energy, saturates at $E_a = 10^{25}$ eV/cm^3 and reaches about 27% that is markedly lower than for heavy ions. However, MgO withstands comparatively high fluences of light ions (around 10^{15} ions/cm^2) which are not allowed in the case of heavy ions. As shown for Kr ions, the depth profile of hardness in the tail part of range displays a maximum where hardness reaches high values (Fig. 7b). The hardening *vs.* absorbed energy curve for Kr ions based on hardness data near the end of range is presented in Fig. 7a (curve 3). At fluence $\Phi = 10^{15}$ Kr/cm^2, which ensures $E_a = 10^{26}$ eV/cm^3, the hardening effect reaches values typical for heavy ions.

4. Conclusion

The presence of single and complex color centers, defect aggregates and ion-induced dislocations have been observed in MgO crystals irradiated with GeV energy heavy ions (^{238}U, ^{209}Bi, ^{197}Au). The accumulation of extended defects under severe irradiation leads to an increase of hardness (up to 40–45%) and a decrease of dislocation mobility (up to 80%). The depth profiles of hardness show also the non-uniformity of damage along the ion path. Such heterogeneity of structure leads to formation of stress gradients which can affect the mechanical properties at macroscopic scale.

The comparison of the results for heavy ions with those obtained earlier for light projectiles [20] shows stronger damage under heavy

ions. However, strong hardening in the end part of the range can be reached also by light ions at higher fluences (not allowed for heavy ions) due to the contribution of nuclear loss mechanism.

The comparison of the depth profiles of damage in radiation-resistant MgO and radiation sensitive LiF shows that despite quantitative differences in ion-induced effects the damage behavior in many aspects is similar:

- The damage in the major part of ion range is dominated by the electronic stopping mechanism. An exception is the end-of-range region where at high-fluence irradiation (10^{13}–10^{15} ions/cm^2) the contribution of the nuclear energy loss mechanism to the creation of dislocations and luminescent aggregate defects becomes notable.
- It is suggested that ion-induced dislocations and aggregate defects in both cases play the main role in the modification of mechanical properties (hardness and dislocation mobility).
- After severe irradiation, the dislocation mechanism of plastic deformation becomes exhausted due to the immobilization of dislocations by extended defects, and both MgO and LiF at indentation behave like amorphous solids.

The results characterize MgO as a radiation resistant material which survives severe irradiation with GeV energy heavy ions at fluences up to 7×10^{13} ions/cm^2, maintains integrity, crystallinity and micro-plasticity, and possesses ion-induced increase of hardness.

Declaration of Competing Interest

The authors declare that they have no known competing financial interests or personal relationships that could have appeared to influence the work reported in this paper.

Acknowledgements

This work has been performed within the framework of the EUROfusion Enabling Research project: ENR-MFE19.ISSP-UL-02 “Advanced experimental and theoretical analysis of defect evolution and structural disordering in optical and dielectric materials for fusion applications”. The views and opinions expressed herein do not necessarily reflect those of the European Commission.

Data availability

The raw/processed data required to reproduce these findings cannot be shared at this time as the data also forms part of an ongoing study.

References

[1] M. Beranger, P. Thevenard, R. Brenier, E. Balanzat, Defect creation by electronic processes in MgO bombarded with GeV heavy ions, Mat. Res. Soc. Symp. Proc. 395 (1996) 365–370.
[2] A. Lushchik, C. Lushchik, A.I. Popov, K. Schwartz, E. Shablonin, E. Vasil’chenko, Influence of complex impurity centres on radiation damage in wide-gap metal oxides, Nucl. Instrum. Methods B 374 (2016) 90–96.
[3] N. Itoh, A.M. Stoneham, Materials Modification by Electronic Excitation, Cambridge University Press, Cambridge, 2001.
[4] L.W. Hobbs, A.E. Hughes, D. Pooley, A study of interstitial clusters in irradiated alkali halides using direct electron microscopy, Proc. R. Soc. Lond. A 332 (1973) 167–185.
[5] F.W. Clinard, G.F. Hurley, L.W. Hobbs, Neutron irradiation damage in MgO, Al_2O_3 and $MgAl_2O_4$ ceramics, J. Nucl. Mater. 108 (109) (1982) 650–670.
[6] R.S. Averback, P. Ehrhart, A.I. Popov, A. von Sambeek, Defects in ion implanted and electron irradiated MgO and Al_2O_3, Radiat. Eff. Defects Solids 136 (1–4) (1995) 169–173.
[7] M.A. Monge, R. Gonzalez, J.E. Santiuste, R. Pareja, Y. Chen, E.A. Kotomin, A.I. Popov, Photoconversion and dynamic hole recycling process in anion vacancies in neutron-irradiated MgO crystals, Phys. Rev. B 60 (1999) 3787–3791.
[8] M.A. Monge, R. Gonzalez, J.E. Santiuste, R. Pareja, Y. Chen, E.A. Kotomin, A.I. Popov, Photoconversion of F^+ centers in neutron-irradiated MgO, Nucl. Instrum. Methods B 166–170 (2000) 220–224.
[9] L.L. Horton, J. Bentley, M.B. Lewis, Radiation damage in ion-irradiated MgO, Nucl. Instrum. Methods B 816 (1986) 221–229.
[10] C. Kinoshita, K. Hayashi, S. Kitajima, Kinetics of point defects in electron irradiated MgO, Nucl. Instrum. Methods B 1 (1984) 209–218.
[11] A. Lushchik, C. Lushchik, K. Schwartz, F. Savikhin, E. Shablonin, A. Shugai, E. Vasil’chenko, Creation and clustering of Frenkel defects at high density of electronic excitations in wide-gap materials, Nucl. Instrum. Methods B 277 (2012) 40–44.
[12] S.J. Zinkle, V.A. Skuratov, Track formation and dislocation loop interaction in spinel irradiated with swift heavy ions, Nucl. Instrum. Methods B 141 (1998) 737–746.
[13] I. Manika, J. Maniks, Swift-ion-induced hardening and reduction of dislocation mobility in LiF crystals, J. Phys. D: Appl. Phys. 41 (2008) 074008.
[14] J. Ohta, K. Suzuki, T. Suzuki, High-resolution electron microscopy of dislocations of MgO, J. Mater. Res. 9 (1994) 2953–2958.
[15] P. Thevenard, M. Beranger, B. Canut, S.M.M. Ramos, N. Bonardi, G. Fuchs, Defects and phase change induced by giant electronic excitations with GeV ions and 30MeV cluster beam, Mat. Res. Soc. Symp. Proc. 439 (1997) 721–726.
[16] S. Moll, Y. Zang, A. Debelle, L. Tome, J.P. Crocombette, Z. Zihua, J. Jagielski, W.J. Weber, Damage processes in MgO irradiated with medium-energy heavy ions, Acta Mater. 88 (2015) 314–322.
[17] A. Dauletbekova, J. Maniks, I. Manika, R. Zabels, A.T. Aklibekov, M.V. Zdorovets, Y. Bikert, K. Schwartz, Color centers and nanodefects in LiF crystals irradiated with 150 MeV Kr ions, Nucl. Instrum. Methods B 286 (2011) 56–60.
[18] A.S. Keh, Dislocations in indented magnesium oxide crystals, J. Appl. Phys. 31 (1960) 1538–1545.
[19] J. Amodeo, S. Merkel, C. Tromas, P. Carrez, S. Korte-Kerzel, P. Cordier, J. Chevalier, Dislocations and plastic deformation in MgO crystals: a review, Crystals 8 (6) (2018) 1–53.
[20] R. Zabels, I. Manika, K. Schwartz, J. Maniks, R. Grants, M. Sorokin, M. Zdorovets, Depth profiles of indentation hardness and dislocation mobility in MgO single crystals irradiated with swift ^{84}Kr and ^{14}N ions, Appl. Phys. A 120 (2015) 167–173.
[21] J.F. Ziegler, J.P. Biersack, U. Litmark, The Stopping and Range of Ions in Solids, Pergamon Press, New York, 1985.
[22] I. Manika, R. Zabels, J. Maniks, K. Schwartz, R. Grants, T. Krasta, A. Kuzmins, Formation of dislocations in LiF irradiated with ^{3}He and ^{4}He ions, J. Nucl. Mater. 507 (2018) 241–247.
[23] W.C. Oliver, G.M. Pharr, An improved technique for determining hardness and elastic modulus using load and displacement sensing indentation experiments, J. Mater. Res. 7 (1992) 1564–1583.
[24] G. Feng, W.D. Nix, Indentation size effect in MgO, Scr. Mater. 51 (2004) 599–603.
[25] T. Harada, Etchant for revealing dislocations in magnesium oxide single crystals, J. Cryst. Growth 44 (1978) 635–637.
[26] D. Caceres, I. Vergara, R. Gonzalez, Y. Chen, E. Alves, Nanoindentation on neutron irradiated MgO crystals, Nucl. Instrum. Methods B 191 (2002) 178–180.
[27] R. Gonzalez, Y. Chen, R.M. Sebek, G.P. Williams, R.T. Williams, W. Gellermann, Properties of the 800-nm luminescence band in neutron-irradiated magnesium oxide crystals, Phys. Rev. B 43 (1991) 5228–5233.
[28] Y. Chen, R.T. Williams, A.B. Sibley, Defect cluster centers in MgO, Phys. Rev. 182 (1968) 960–964.
[29] V. Skvortsova, L. Trinkler, Luminescence of impurity and radiation defects in magnesium oxide irradiated by fast neutrons, Phys. Procedia 2 (2009) 567–570.
[30] A. Dauletbekova, V. Skuratov, N. Kirilkin, I. Manika, J. Maniks, R. Zabels, A. Akilbekov, A. Volkov, M. Baizhumanov, M. Zdorovets, A. Seitbayev, Depth profiles of aggregate centers and nanodefects in LiF crystals irradiated with 34 MeV 84Kr, 56 MeV 40Ar and 12 MeV 12C ions, Surf. Coat. Technol. 355 (2018) 16–21.
[31] I. Manika, J. Maniks, K. Schwartz, M. Toulemonde, C. Trautmann, Hardening and long-range stress formation in lithium fluoride induced by energetic ions, Nucl. Instrum. Methods B 209 (2003) 93–97.
[32] A. Richter, B. Wolf, M. Nowicki, R. Smith, I.O. Usov, J.A. Valdez, K. Sickafus, Multi-cycling nanoindentation in MgO single crystals before and after ion irradiation, J. Phys. D: Appl. Phys. 39 (2006) 3342–3349.
[33] Yu.I. Golovin, A.I. Tyurin, Non-dislocation plasticity and its role in mass transfer and imprint formation during dynamic indentation, Solid State Phys. 10 (2000) 1818–1820.
[34] J. Maniks, R. Zabels, I. Manika, Shear banding mechanism of plastic deformation in LiF irradiated with swift heavy ions, IOP Conf. Series: Mater. Sci. Eng. 38 (2012) 012017.
[35] R. Zabels, I. Manika, K. Schwartz, J. Maniks, R. Grants, MeV–GeV ion induced dislocation loops in LiF crystals, Nucl. Instrum. Methods B 326 (2014) 318–321.
[36] I. Manika, J. Maniks, R. Zabels, K. Schwartz, R. Grants, A. Dauletbekova, A. Rusakova, M. Zdorovets, Modification of LiF structure by irradiation with swift heavy ions under oblique incidence, IOP Conf. Series: Mater. Sci. Eng. 49 (2013) 012011.